

Supporting Information

Operando Time and Space-Resolved Liquid-Phase Diagnostics Reveal the Plasma Selective Synthesis of Nanographenes

Darwin Kurniawan,¹ Francesca Caielli², Karthik Thyagajaran², Kostya (Ken) Ostrikov,³ Wei-Hung Chiang,^{1*} and David Z. Pai^{2,4*}

¹Department of Chemical Engineering, National Taiwan University of Science and Technology, Taipei 10607 Taiwan

²Institut Pprime (CNRS-Université de Poitiers-ENSMA), Futuroscope Chasseneuil, F-86962, France

³School of Chemistry and Physics and QUT Centre for Materials Science, Queensland University of Technology (QUT), Brisbane, 4000, Australia

⁴Laboratoire de Physique des Plasmas, CNRS, Sorbonne Université, Université Paris-Saclay, École Polytechnique, Institut Polytechnique de Paris, F-91128, Palaiseau, France

*Corresponding author: E-mail address: david.pai@lpp.polytechnique.fr;
whchiang@mail.ntust.edu.tw (W.H.C)

S1. Experimental section

Materials & chemicals

Low molecular weight chitosan (50 – 190 kDa, CAS: 9012-76-4) and sodium hydroxide (NaOH, CAS: 1310-73-2) were obtained from Sigma Aldrich. Acetic acid glacial (CAS: 64-19-7) was received from Fischer Scientific. Pt foil with a dimension of $20 \times 20 \times 0.1 \text{ mm}^3$ was purchased from Guv Team International.

Synthesis of NGQDs

The colloidal NGQDs was synthesized using an argon atmospheric-pressure microplasma electrochemical reactor which is similar to our previous works.^{1, 2} 62.5 μM of chitosan solution was prepared in 50 mM of aqueous acetic acid, followed with a continuous stirring at 600 rpm for 24 hours to homogenize the solution. Then, the solution was poured into a quartz cuvette until full and subjected to a microplasma reaction at a fixed discharge current of 5 mA for 60 min to synthesized the NGQDs. After the reaction, the solution was neutralized using 1 M NaOH and subsequently followed with the addition of acetone with a volume ratio of 2:1 of that acetone and colloidal NGQDs, respectively. The addition of acetone would precipitate the unreacted chitosan. Then, the suspension was subjected to vacuum filtration to remove the chitosan precipitate. The acetone contained in the filtrated solution was removed using rotary evaporator. Once the acetone has been removed, the colloidal NGQDs was dialyzed against DI water for 2 days to remove the salts and buffers formed during the neutralization. The outer solution was regularly replaced with a fresh DI water for every 6 hours. After the dialysis, the inner solution was rotary evaporated until around 0.5 mL solution left. A little amount of ethanol was added into the solution to precipitate the NGQDs. Finally, fine NGQD powder was obtained after all the mixture had been evaporated.

Characterizations of NGQDs

Ex situ PL measurement of colloidal NGQDs was conducted at room temperature using a commercial Horiba JobinYvon Nanolog-3 spectrofluorometer. *Ex situ* absorption measurement was performed using a JASCO V676 absorbance spectrophotometer. Fourier-transform infrared

(FTIR) measurement was conducted in powder form using a Shimadzu Tracer-100 by mixing 2 – 5 wt% of sample specimen with KBr. Transmission electron microscope (TEM) measurements were performed using a field emission gun TEM (JEOL JEM-2100F) with an accelerating voltage of 200 kV. *Ex situ* microRaman measurement was conducted at room temperature using a JASCO 5100 spectrometer with a laser excitation wavelength of 532 nm. The Raman spectrometer was calibrated with a silicon wafer (Raman shifts: 520 cm^{-1}) before every measurement. Atomic force microscope (AFM) measurements were performed using an Ardic Instrument P-100 AFM in height trace tapping mode. *In situ absorption* measurement was performed using an Ocean Optics HR4000 spectrometer coupled with a UV-VIS light source (Ocean Optics DT-MINI-2-GS Deuterium Tungsten Halogen light source) with a measurement condition of 10 ms integration time and 200 accumulations. Proton nuclear magnetic resonance (^1H NMR) measurements were performed using Bruker Avance III HD-600 MHz NMR. D_2O was used as the solvent for all the measurements. For semi-quantitative analysis, an internal standard solution was prepared by dissolving 10 mg of maleic acid (MA) in 10 mL of D_2O . The chitosan solution was subjected to microplasma treatment at 5 mA for a certain time (15, 30, and 60 min). Immediately after the reaction, the tip of the volumetric pipette was carefully injected into the solution at 2-5 mm depth to take 1.2 mL solution out and moved to a sample vial. Afterwards, a different tip of a volumetric pipette was carefully reinjected into the solution at a depth of 13 mm to take 1.2 mL solution out and moved to a different sample vial. The solutions were evaporated using a rotary evaporator and subsequently added to 1 mL of MA internal standard solution. The mixtures were sonicated for 5 min before taking 0.6 mL out for ^1H NMR measurements. The obtained ^1H NMR spectra were normalized against MA peak at 6.37 ppm to allow semi-quantitative analysis.

PIV measurement

PIV was used to quantify the flow velocity field in the liquid phase, *in situ* during the plasma synthesis of NGQDs. In this work, this technique involved introducing fluorescent tracer particles (VESTOSINT[®] polyamide powder containing Rhodamine 6G, 5 μm mean diameter) into the solution. As shown in Figure S1, a laser sheet produced by a double-pulse laser (Quantel Twins Ultra, 532 nm, 30 mJ per pulse) illuminated the particles found in a vertical plane in the flow, and dual images of the particle distribution were recorded using a camera (Lavision Imager Pro,

2048×2048 pixel sensor array) equipped with an objective lens (Nikon 105 mm) and oriented perpendicularly to the laser direction. Stray light at 532 nm due to laser scattering off the optical cell was eliminated from detection by a 540 nm high-pass filter. Each pair of images represents the particle distribution at two instances separated by 1.2 – 1.5 μ s. The particle displacement can be obtained through PIV analysis software (Lavisision DaVis version 8.4.0) using a double-pass algorithm to calculate the velocity field.

S2. XPS analysis

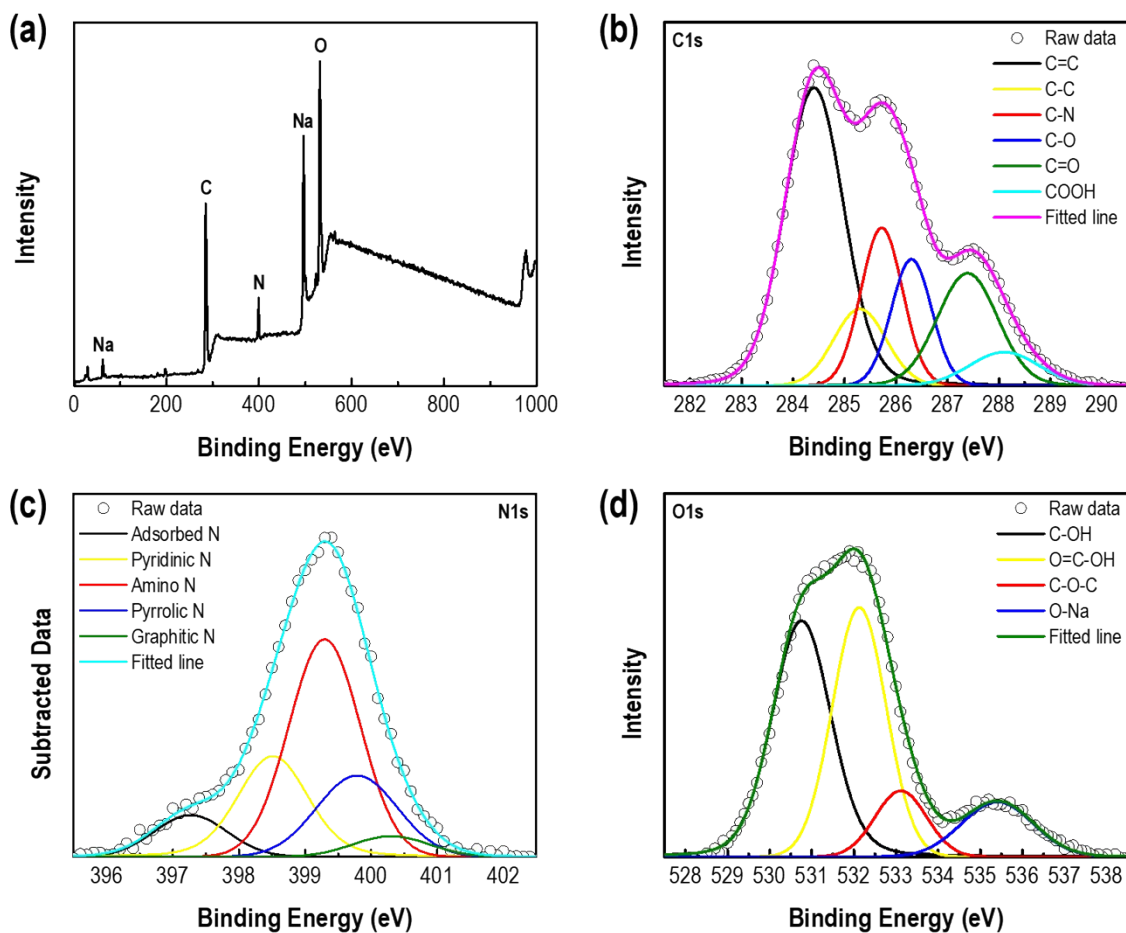


Figure S1. (a) Full XPS survey scan of NGQDs. High-resolution XPS scan on (b) C1s, (c) N1s, and (d) O1s.

Table S1. Elemental composition of the synthesized NGQDs.

Element	Composition (at.%)
C	65.99
N	6.22
O	27.79

S3. AFM analysis

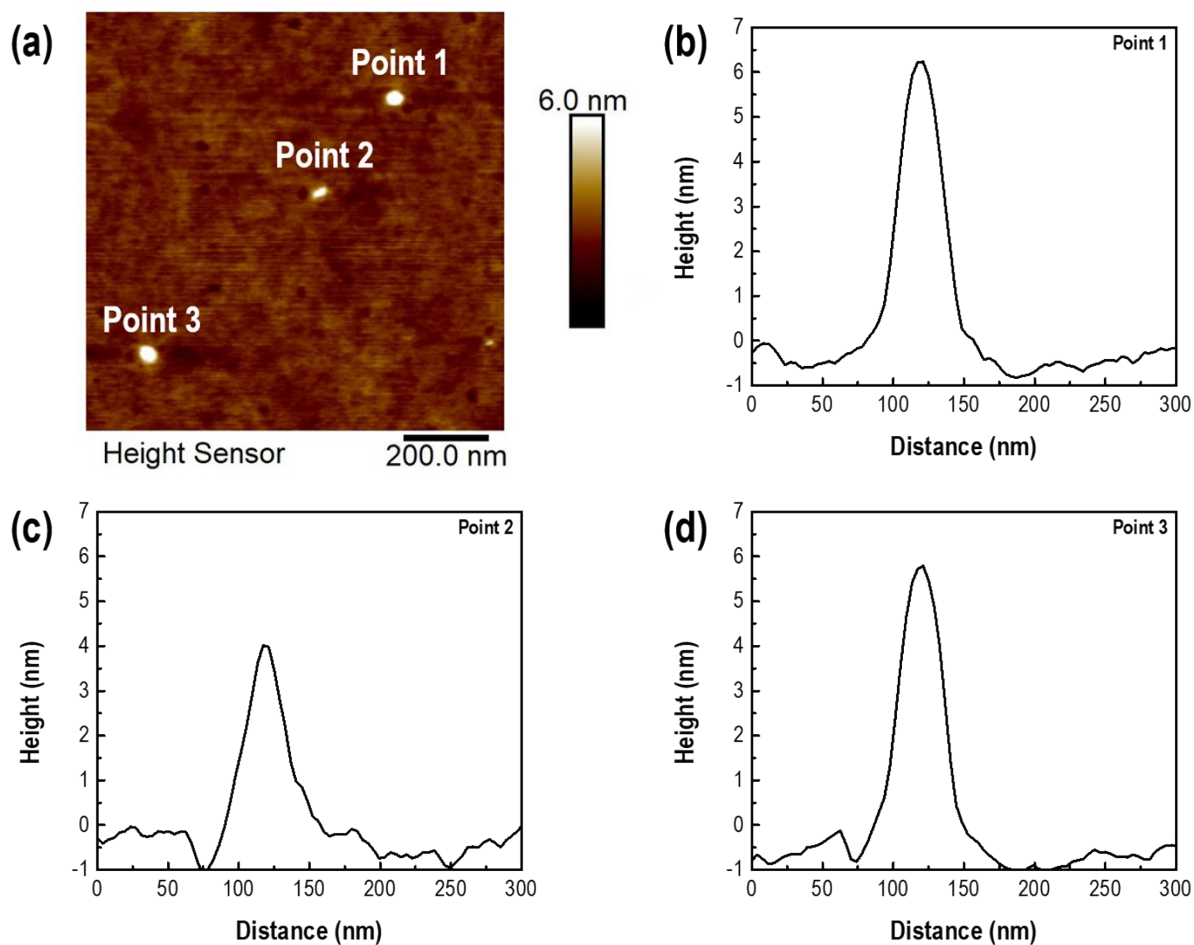


Figure S2. (a) High magnification AFM image of NGQDs and (b)-(d) the corresponding height profile at point 1 – 3, respectively.

S3. *In situ* diagnostics

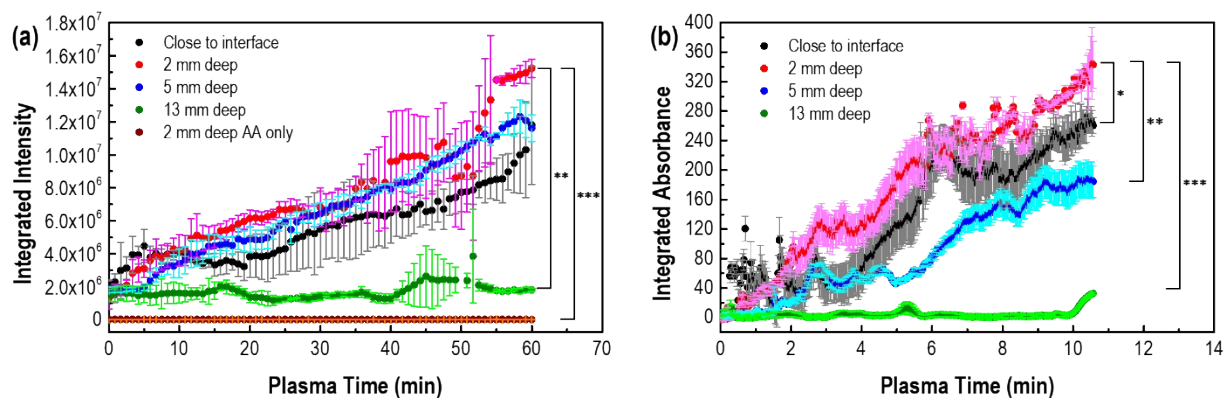


Figure S3. Time series of (a) integrated PL intensity changes at different depths and (b) integrated absorbance from 350 – 550 nm at different depths with error bars ($*p < 0.05$, $**p < 0.01$, $***p < 0.001$; $n = 2$). Acetic acid is denoted as AA.

S4. Electron density

To measure electron number density (n_e), we employed OES using the experimental apparatus described in Ref. 3, which involved using a UV microscope to collect plasma emission and a spectrometer equipped with an intensified CCD camera to acquire the OES spectra. Plasma emission from the hydrogen Balmer line (H_β) was observed during NGQD synthesis and used to calculate n_e .

The spectral data fit a Voigt profile, and upon deconvolution from the instrumental function, the remaining Voigt profile with a full-width at half-maximum (FWHM) of $\Delta\lambda_V$ of about 0.07 nm is the convolution of a Gaussian profile due to Doppler broadening and a Lorentzian profile due to Stark and Van Der Waals (collisional) broadening. The FWHM of the Lorentzian profile ($\Delta\lambda_L$) is the sum of the FWHMs of Lorentzian components due to Stark broadening ($\Delta\lambda_S$) and Van der Waals broadening ($\Delta\lambda_{vdw}$). The FWHM of the Gaussian profile due to Doppler broadening ($\Delta\lambda_D$) is estimated to be 0.02 nm according to $\Delta\lambda_D = 3.48 \times 10^{-4} T^{0.5}$, calculated for the case of air in Ref. 4, where the gas temperature T is assumed to be 3250 K, which was the value found for an air discharge generated over water 5 Given that $\Delta\lambda_V$ is about 0.07 nm, the approximate

$$\Delta\lambda_L = \frac{\Delta\lambda_V^2 - \Delta\lambda_D^2}{\Delta\lambda_V} \quad \text{discussed in Ref. 6 yields } \Delta\lambda_L = 0.064 \text{ nm.}$$

Assuming that Van der Waals broadening is similar in air and the air-argon mixture studied here, this contribution is estimated to be $\Delta\lambda_{vdw} = 0.0125$ nm according to $\Delta\lambda_{vdw} = 3.6P/T^{0.7}$, derived in Ref. [4] for pure air, where the pressure P is 1 atm and assuming $T = 3250$ K. The Stark component $\Delta\lambda_S = \Delta\lambda_L - \Delta\lambda_{vdw}$ is related to n_e according to Ref. 7:

$$\Delta\lambda_S = 4.7351 \left(\frac{n_e}{10^{23}} \right)^{0.69052}$$

Where $\Delta\lambda_S$ and n_e are expressed in nm and m^{-3} , respectively. The Stark broadening of the Lorentzian profile corresponds to a value of $n_e \approx 1 \times 10^{14} \text{ cm}^{-3}$.

S5. PIV setup

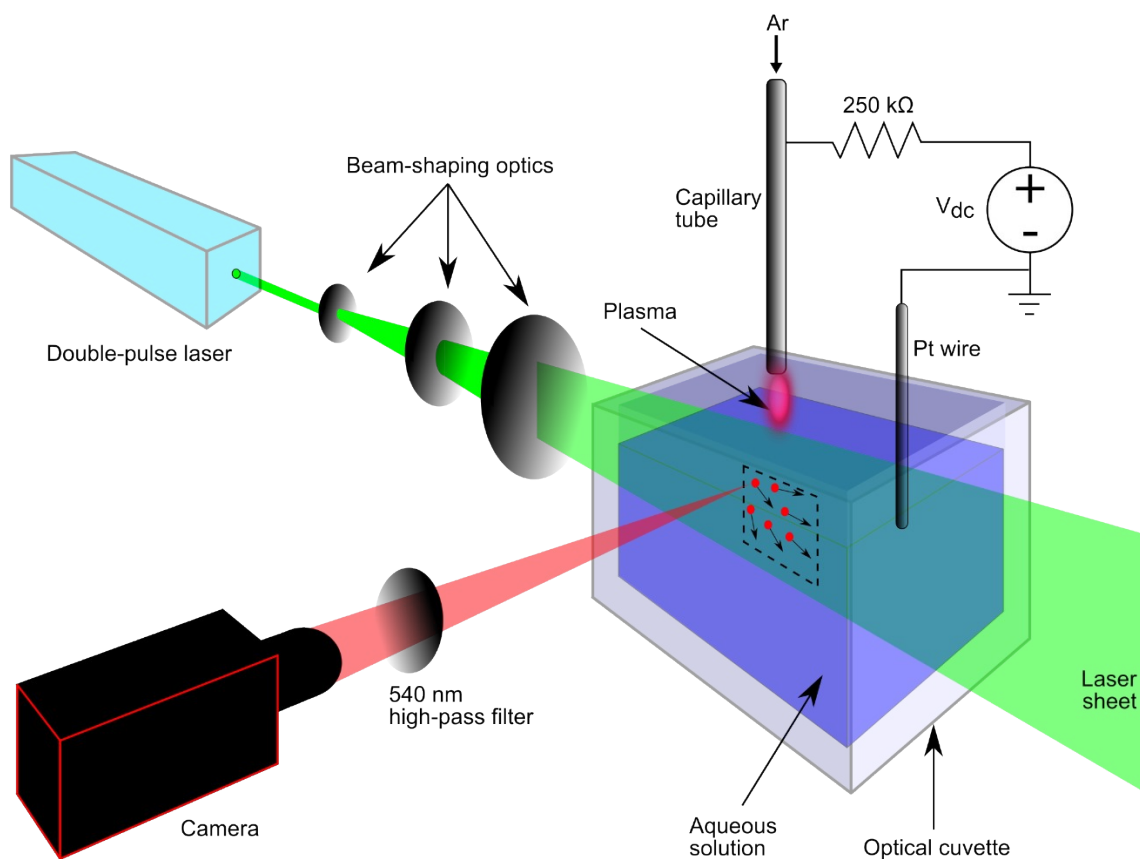


Figure S4. Schematic diagram of experimental setup for PIV. Shown are the laser and optics for shaping the laser beam into a sheet positioned underneath the plasma. The optics consist of a beam expander and a cylindrical lens, which created a laser sheet that fully illuminated a vertical cross section of the optical cell. Underneath the plasma is an example interrogation window containing tracer particles tracking the liquid flow, with the fluorescence from one of the particles captured by the camera.

S6. ^1H NMR measurements

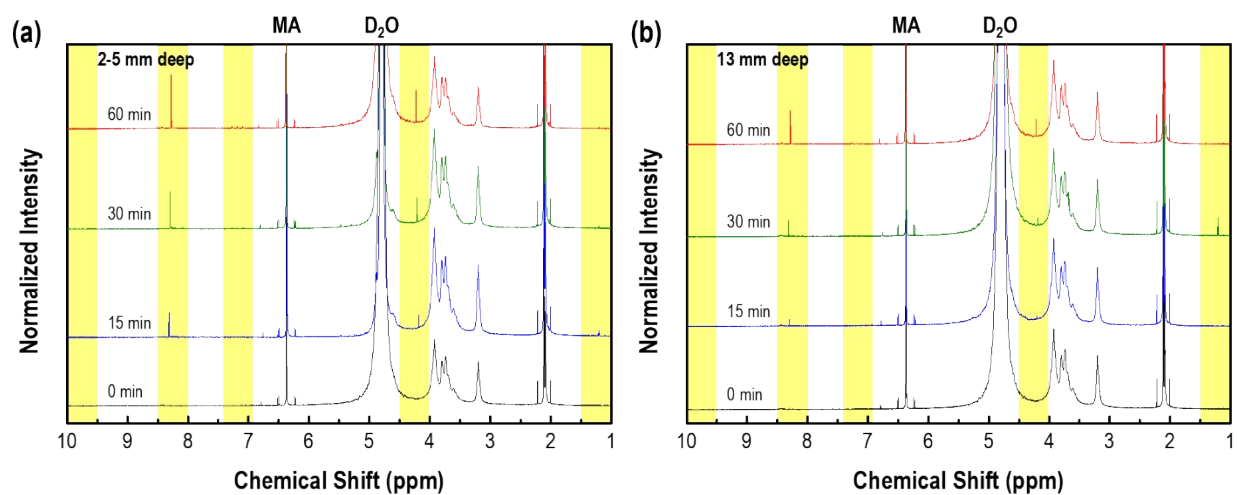


Figure S5. Full ^1H NMR spectra in the range of 1 – 10 ppm of chitosan solution located at (a) 2-5 mm and (b) 13 mm deep into the solution after 0, 15, 30, and 60 min of plasma treatment at 5 mA fixed discharge current.

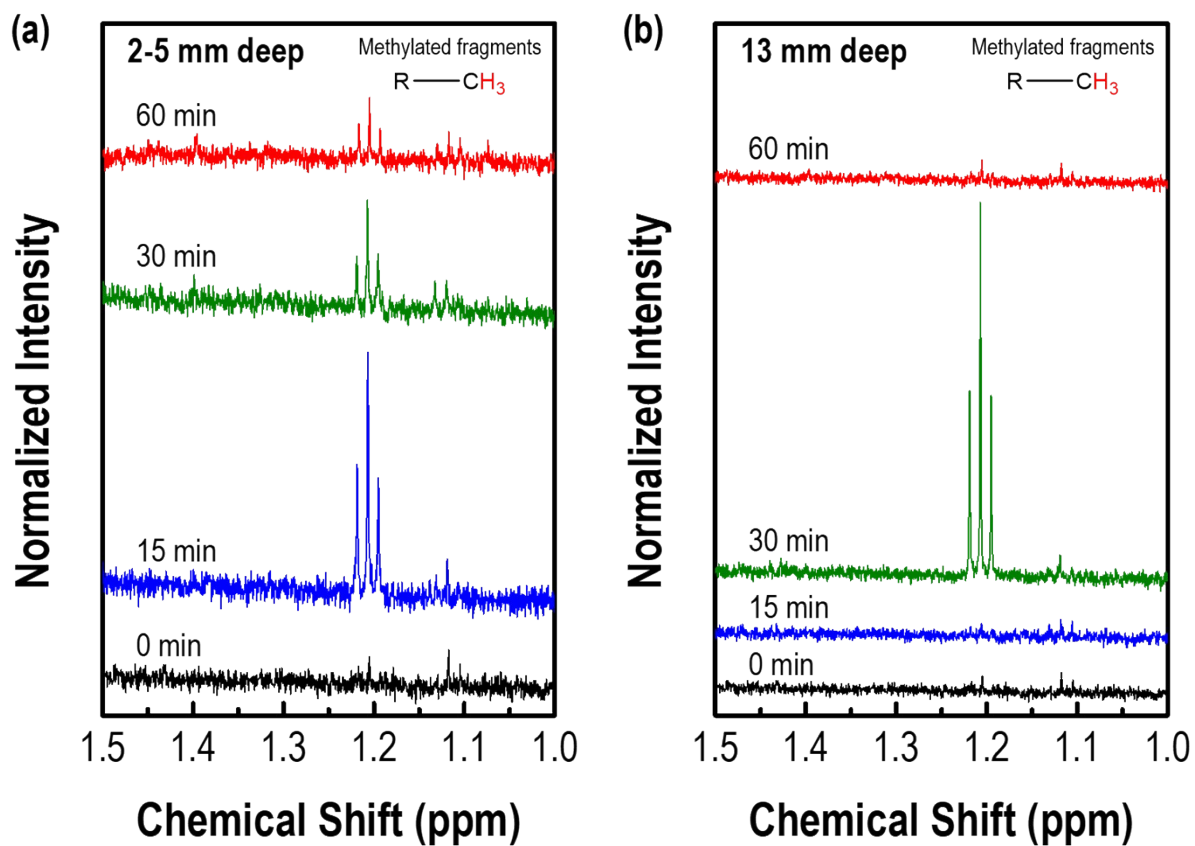


Figure S6. Magnification of ¹H NMR spectra in the range of 1.0 – 1.5 ppm of chitosan solution located at (a) 2-5 mm and (b) 13 mm deep into the solution after 0, 15, 30, and 60 min of the plasma treatment at 5 mA fixed discharge current.

S7. Scavenging of plasma-generated reactive species

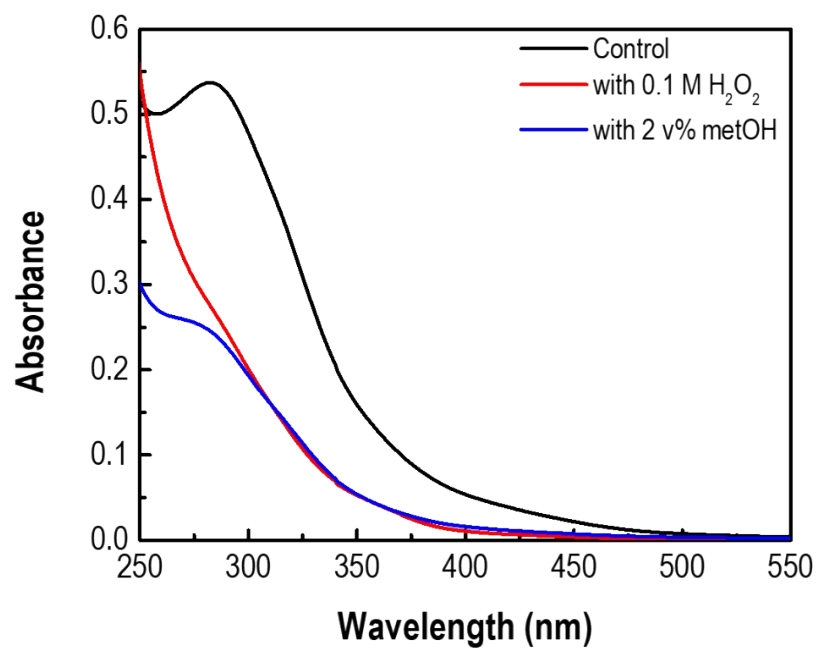


Figure S7. Absorption spectra of the plasma-treated chitosan solution without the addition of reactive species scavengers (blank) and with the addition of 0.1 M H₂O₂ as solvated electron (red) and 2 v% of methanol as OH radical (blue) scavengers.

References

1. Kurniawan, D.; Chiang, W.-H., Microplasma-Enabled Colloidal Nitrogen-Doped Graphene Quantum Dots for Broad-Range Fluorescent pH Sensors. *Carbon* **2020**, *167*, 675-684.
2. Kurniawan, D.; Jhang, R.-C.; Ostrikov, K. K.; Chiang, W.-H., Microplasma-Tunable Graphene Quantum Dots for Ultrasensitive and Selective Detection of Cancer and Neurotransmitter Biomarkers. *ACS Appl. Mater. Interfaces* **2021**, *13* (29), 34572-34583.
3. Darny, T.; Babonneau, D.; Camelio, S.; Pai, D. Z., Uniform Propagation of Cathode-Directed Surface Ionization Waves at Atmospheric Pressure. *Plasma Sources Sci. Technol.* **2020**, *29* (6), 065012.
4. Laux, C. O.; Spence, T. G.; Kruger, C. H.; Zare, R. N., Optical Diagnostics of Atmospheric Pressure Air Plasmas. *Plasma Sources Sci. Technol* **2003**, *12*, 125–138.
5. Verreycken, T.; Schram, D. C.; Leys, C.; Bruggeman, P., Spectroscopic Study of an Atmospheric Pressure DC Glow Discharge with a Water Electrode in Atomic and Molecular Gases. *Plasma Sources Sci. Technol.* **2010**, *19* (4), 045004.
6. Whiting, E. E., An Empirical Approximation to the Voigt Profile. *J. Quant. Spectrosc. Radiat. Transfer* **1968**, *8* (6), 1379-1384.
7. Dardaine, N. Estimation de la densité électronique dans les plasmas froids d'air à pression atmosphérique grâce à l'effet Stark. Université de Poitiers, 2017.